NASA Technical Memorandum 87094

Coupled Aerodynamic and Acoustical Predictions for Turboprops

(NASA-TM-87094) COUPLED AERODYNAMIC AND ACOUSTICAL PREDICTIONS FOR TURBOPROPS (NASA) 13 p Avail: NTIS HC A02/MF A01 CSCL 01A

N87-23598

Unclas H1/02 0080190

Bruce J. Clark and James R. Scott
Lewis Research Center
Cleveland, Ohio

LIBRARY COPY

APR 1 1987

LANGLEY RESEARCH CENTER
LIBRARY, NASA
HAMPTON, VIRGINIA

Prepared for the
One hundred and seventh Meeting of the American Acoustical Society
Norfolk, Virginia, May 7–10, 1984

NASA

Summary

To predict the noise fields for proposed turboprop airplanes, an existing turboprop noise code by Farassat has been modified to accept blade pressure inputs from a three-dimensional aerodynamic code. An Euler-type code written by Denton can handle the nonlinear transonic flow of these high-speed, highly swept blades. This turbofan code of Denton's was modified to allow the calculation mesh to extend to about twice the blade radius and to apply circumferential periodicity rather than solid-wall boundary conditions on the blade in the region between the blade tip and the outer shroud. Outputs were added for input to the noise prediction program and for color contour plots of various flow variables. The Farassat input subroutines were modified to read files of blade coordinates and predicted surface pressures. Aerodynamic and acoustic results are shown for the SR-3 model blade. Comparison of the acoustic predicted results with measured data shows good agreement.

Introduction

The pressures for more fuel-efficient flight have forced a reconsideration of propeller-driven commercial aircraft. The turboprops being considered have highly swept blades and operate with supersonic tip speeds to achieve the necessary characteristics for a Mach 0.8 cruise condition. A prediction procedure for the noise generated by the propeller is needed to assess not only the cabin noise environment but also the community noise impact. Such a procedure has been written by Farassat (ref. 1) of Langley Research Center based on the Ffowcs-Williams—Hawkings equation for source strength. It is programmed to compute the contributions to the noise field due to thickness, loading, and surface drag of the propeller blade. This report presents a method of providing the pressure distributions on the blade surfaces. These distributions are necessary to calculate the loading noise.

Although isolated data are available from laser velocity and implanted-transducer surface pressure measurements, they are inadequate for characterizing the source strengths over the blade. Several three-dimensional aerodynamic codes now exist for calculating the steady flow around a blade, including the static pressure. For transonic turboprop applications, a code must be able to handle the nonlinear effects of shocks. Because of the large amount of sweep in these blades, it is important that the code be three-dimensional to predict radial flow effects. Presently available codes do not include viscous terms and do not allow for flow separation. They are generally based on the Euler formulation of the equations of mass, momentum, and energy conservation.

Denton, of the University of Cambridge, has written one of these codes for a turbofan stage (ref. 2), and it has been modified and made operational on the Cray 1-S computer at Lewis Research Center. It uses a time-marching solution of the equations for conservation of mass, energy, and three components of momentum in a rotating cylindrical coordinate system. An input mesh must be supplied with sufficient mesh points to define the anticipated flow characteristics.

Modifications are made to the boundary conditions of this Denton code to account for a blade extending only part of the way to the outer mesh surface. Output modifications are made for the inputs necessary for the Farassat noise code and for added color contour plotting routines.

The Denton code includes an option to bleed flow through the solid surfaces in the flow field to simulate the effects of boundary layers. This feature of the program is still being adapted for turboprop calculations and is not yet implemented.

The inputs for the Farassat program are in the form of subroutines for the blade geometry and for the blade pressure distributions. These subroutines were modified to read files of manufacturer's coordinates for the blade shape and to read the output file from the Denton code.

These coupled aerodynamic and acoustic codes are applied to the flow and noise calculations for a modern transonic turboprop blade. Results are compared to other flow predictions and to measured acoustic data.

Description of Modified Denton Code

Denton's scheme for solving the Euler equations uses a finite-volume, time marching solution of the equations of continuity, axial, radial, and circumferential momentum and energy. In his approach the flow quantities are *forward marching* (i.e., changes propagate in the direction of flow), while the pressure is *upstream marching*. In each volume element the changes in momentum and energy are applied to the downstream corners of the element. Pressure corrections with damping are applied to the downstream pressures to get an upstream *effective pressure*.

An input mesh must be supplied with adequate fineness of spacing to resolve gradients near the leading and trailing edges

and in regions where shocks might occur. The mesh lines must be continuous and have smooth transitions. Denton suggests limiting the changes in relative spacing between adjacent mesh lines to 25 percent because of the smoothing routines used. The mesh must extend far enough upstream and downstream of the blades so that the flow properties can be defined at the extremes. The mesh defines the geometry of both sides of the blade and is given in cylindrical coordinates (axial, X; radial, R; and tangential, $R\theta$) for the suction surface of the blade, with blade thicknesses given at each mesh point (in $R\,\Delta\theta$) to define the pressure surface of the blade. In the radial direction, the mesh must encompass the blade cross sections out to the tip, and additional mesh is necessary for the flow field between the blade tip and the "fan casing" at the last radial position. This last provision represents a modification to the fan code for turboprop applications. From the input mesh the Denton code generates its own interpolated three-dimensional mesh spacing in both the radial and circumferential directions.

Boundary conditions are applied on all solid surfaces of the blade, hub, and on the phantom outer casing. Fluxes through those surfaces are zeroed on each updating. The code has been modified to recognize that the blade does not extend to the outer casing. Boundary conditions of periodicity are applied before and behind the blades and, in this modified form, beyond the blade tip. Flow variables at the first and last circumferential mesh points are equated to the average of the two in these regions of the flow field.

Required inputs to the code include the total temperature (TO1) and pressure (PO1) at the upstream end of the flow field. These values, of course, are corrected for the altitude and flight speed of the aircraft. The gas specific heat and specific heat ratio and the rotational speed of the propeller are also required inputs. The size of the propeller is defined by the radial coordinates of the meridional mesh line representing the blade tip. Other radial mesh lines are identified as the leading and trailing edges of the blade.

At the inlet several options are available as boundary conditions on the swirl velocity and radial velocity. For turboprop applications the appropriate options fix the absolute swirl velocity and the meridional gradient of the radial velocity at zero at the inlet.

Several input options control the stability and rate of convergence of the solution. The prime stability control is the choice of a multiplier for the time-step size. Other choices include the amount of pitchwise and spanwise smoothing and a damping factor to control the amount of negative feedback in each iteration. Suitable values of these parameters must be found by experience. A small change in the time-step multiplier c_{mult} substantially affect the convergence rate. Denton suggests typical values for each of these inputs. Some of the Denton inputs required and the calculation parameter inputs are listed in table I.

Although the Denton code contains numerous options for printing maps of various flow variables of interest, it was necessary to add other write statements to generate files for plotting and for input to the Farassat code. At Lewis Research Center a plotting routine has been developed (ref. 3) to generate color contours of flow variables such as pressure, Mach number, and velocities. This plotting routine has been used in generating the color contour plots shown later. A separate plotting code is used for the pressure survey plots shown later. Each routine requires a separate output file. For the color graphics a full set of mesh coordinates (in R, θ, and X) is written followed by arrays of flow variable quantities desired for plotting. For input to the line profile pressure plots, generalized flow variables (ρ, ρV_x, ρV_r, ρV_θ, ρE) are written for each mesh point, and the pressures or other flow variables desired are reconstructed in a separate part of the plotting package. Mesh coordinates are also reconstructed from the data input to the Denton calculation. The file to be read by the Farassat code consists of arrays of radial and axial blade surface coordinates and arrays of pressures on each side of the blade.

Because of the long calculation times involved in both the Denton and Farassat programs, it was decided to keep the calculations separate so that the aerodynamic results could be examined for consistency and satisfactory convergence before the acoustic calculations were begun. A typical solution time for the detailed flow field around a turboprop blade is about 1000 sec of CPU time on the Cray 1-S computer.

Description of Modified Farassat Code

The approach chosen by Farassat for the turboprop noise calculation provides for the integration of both the near- and far-field contributions from the blade panels, which are either subsonic or supersonic with respect to the observer. For these two conditions separate formulations of the basic Ffowcs-Williams—Hawkings equation are used. Quadrupole terms are omitted in this approach; hence, blade surface dipoles are the assumed sources. Separate integrations are made of the loading (surface pressure dependent), drag (surface drag dependent), and thickness (shape dependent) contributions to the total noise. In the version of Farassat's program that we have used, the derivatives in the Ffowcs-Williams—Hawkings equation are taken by differencing after the integrations have been performed. A newer version of the program takes these derivatives inside the integral, thus introducing less machine noise in the calculation. From these integrations, separate time histories are constructed of the loading, thickness, and drag contributions and of their sum. Each history is then Fourier transformed to get spectra for each component and the total.

The geometry of the blade is specified at cuts made perpendicular to the pitch change axis of the blade. At each cut, the leading-edge displacement, twist angle, chord, and thickness are required. At each cut the blade cross section coordinates are also required as a function of percent of chord. These blade coordinates are read in two subroutines in the Farassat code. These coordinates are used to locate individual

TABLE I.—DENTON CODE INPUTS

(Modified, with some unused options omitted.)

Code	Definition
	Grid
IM, JM, KM	Number of grid nodes pitchwise (I), streamwise (J), and spanwise (K)
JLE, JTE	Mesh lines of J corresponding to leading and trailing edges
KTIP	Mesh line in K passing through blade tip
NOSECT	Number of spanwise points in input geometry of blade
FP, FR	Factors for relative grid spacing, pitchwise and spanwise
	Flow field
NBLADE	Number of blades
RPM	Propeller rotational speed
CP, GA	Gas specific heat and specific heat ratio
PO1, TO1	Total pressure and temperature at inlet (J = 1) for each K
PDHUB	Static pressure at downstream hub surface (J = JM, K = 1)
VTIN	tangential (pitchwise) velocity component at inlet for each K, initial guess
VMI	Meridional velocity component at inlet for each K, initial guess
BS	Swirl angle at inlet for each K
INMACH	Set = 0 to fix absolute flow angle at inlet at BS value
INVR	Set = 0 to fix inlet radial velocity gradient to 0 in meridional direction
	Computational variables
NMAX	Maximum number of time steps
ITIMST	Set = 1 for nonuniform time steps based on dimension of each element
FT	Time step multiplying factor
ISMTH	Set = 1 for linear smoothing of SF, pitchwise and spanwise
SF	Smoothing factor in pitchwise and spanwise directions
RF	Relaxation factor on pressure correction
FUP	Magnitude of pressure correction factor
DAMP	Negative feedback factor
	Output options
IOUT	Controls selection of variables to be printed in output
PLOT	Logical variable for writing file for survey plots of flow variables
COLOR	Logical variable for writing file for color contour plots

panels into which the blade surfaces are subdivided for integrating the noise.

The file of mesh points and corresponding blade surface pressures generated by the Denton code are read in the Farassat input subroutine for pressure. A two-dimensional linear interpolation routine is used to obtain the pressure at the particular locations required by the Farassat calculation. The pressures are in normalized form and are converted into the proper dimensions following the interpolation by multiplying by the local relative velocity head on the blade (half the density times the sum of the squares of the flight velocity and local wheel speed).

In addition to files from the Denton output, the usual inputs are required for the Farassat code for various blade and operating parameters. Ideally, these should exactly duplicate the parameter values used for the Denton code input. However, since the pressures have been normalized, the Farassat solution can be obtained over a limited range of parameters, as long as the character of the flow does not change. The user can modify the pressures on the blade by choosing a multiplier PFACTOR so that the predicted aerodynamic performance will match an experimental value. Since this changes the pressures on the blade, it will also directly affect the noise to some degree. The operating parameter inputs and calculation option inputs for the Farassat code are listed in table II.

Considerable computational time may be required to predict the noise levels at a number of observer stations, since each station requires a separate calculation. For subsonic calculations the formulation does not require the trial and error calculation for the correct retarded time, and solutions times are relatively short. The solution time is much longer when the blade tip is moving supersonically with respect to the

OF POOR QUALITY

TABLE II.—MODIFIED FARASSAT CODE INPUTS

Code	Definition
C	Speed of sound
DENTON	Logical variable to call for reading Denton code output
EPSILON	Maximum allowable error in retarded time calculation
FRACDT	Fraction of time step to use for differentiation
INDENT	Alphanumeric identifier for title
MOTION	Logical variable to move observer forward with propeller
MTRANS	Transition Mach number for using supersonic subroutines
NBLADES	Number of blades
NCF	Factor to increase the number of chord divisions when supersonic
NLE	Number of chord divisions from leading edge to THKMAXL
NPCA	Number of span divisions of the blade
NPCAF	Factor to increase the number of span divisions when supersonic
NPTS	Number of time points per blade passing period
NSPEC	Number of tone harmonics to calculate
NTAU	Number of time divisions in collapsing sphere routing
NTE	Number of chord divisions from THKMAXL to trailing edge
R	Outer blade radius
REV	Rotational blade speed, rpm
RHO	Air density
RINNER	Blade radius at hub
THKMAXL	Chordwise location of transition from NLE Spacing to NTE spacing
TRANS	Transition Mach number to omit Doppler shift term
V3	Forward speed of propeller
XO(1)	Observer distance perpendicular to pitch axis in propeller plane
XO(2)	Observer distance along pitch axis in propeller plane
XO(3)	Observer distance ahead in direction of propeller axis

observer. At stations well ahead or behind the plane of the propeller, the relative motion is usually subsonic, and solutions are obtained in about 25 percent of the time required for supersonic relative motion.

Application to Turboprop Noise Calculation

The model propeller configuration SR-3 manufactured by Hamilton-Standard is an example of a modern, highly swept, transonic turboprop (fig. 1). This model has been tested extensively in wind tunnels (refs. 4 and 5) and in flight (ref. 6) for its acoustic and aerodynamic performance. Limited measurements of the detailed flow field around the blades have been made using a laser velocimeter (ref. 7). Flow field and acoustic predictions for the SR-3 blade have been made using the Denton and Farassat codes for studies in support of other advanced turboprop designs. Some of the results of these calculations are presented here to illustrate the technique and value of coupling these codes.

The SR-3 model propeller has 8 blades and is 0.622 m (24.5 in) in diameter, with approximately 45° of sweep at the tip. The maximum blade chord is about 20 percent of the diameter, and the twist is 41° from hub to tip. Design conditions for the propeller were for 0.8 flight Mach number at a 10 671-m (35 000-ft) altitude, a power loading of 301 kW/m^2 (37.5 SHP/ft^2), and a speed of 7348.5 rpm. The design blade angle at 3/4 radius is 61.3°, which untwists to 58.7° with centrifugal loading at design speed. The design conditions used for the calculations are summarized in table III.

Aerodynamic Calculations

The computational grid for these calculations consisted of 41 streamwise (axial), 32 spanwise (radial), and 11 pitchwise

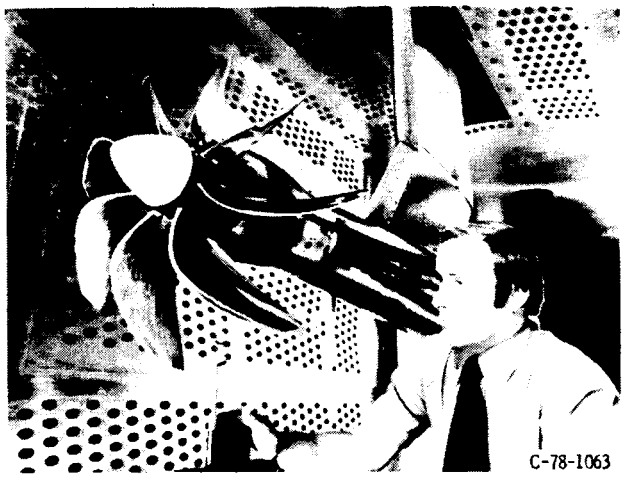

Figure 1.—Propeller SR-3 in tunnel.

TABLE III.—SR-3 TURBOPROP DESIGN OPERATING CONDITIONS

Altitude, m (ft)	10 670.7 (35 000)
Temperature, K (°F)	219.0 (-65.8)
Pressure, N/m^2 (lb/ft^2)	23 839.6 (497.9)
Density, kg/m^3 ($slugs/ft^3$)	0.3798 (0.000737)
Flight Mach number	0.8
Tip rotational speed, m/sec (ft/sec)	243.9 (800)
Tip rotational Mach number	0.8223
Tip relative Mach number	1.1473
Advance ratio	3.0563
Disk loading, kW/m^2 (SHP/ft^2)	301 (37.5)
Power coefficient	1.6951
Diameter, m (ft)	0.634 (2.0792)
Rotational speed, rpm	7348.5

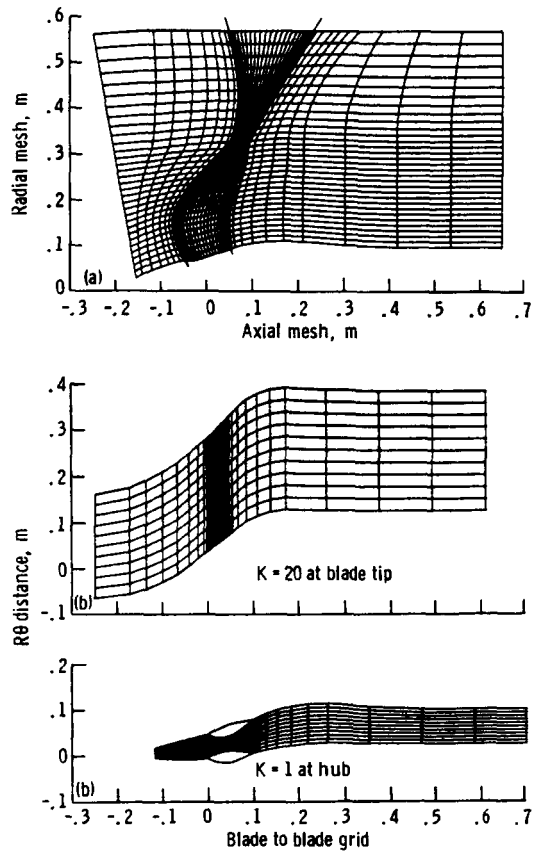

(a) Meridional direction.
(b) Pitchwise distribution.

Figure 2.—Computational mesh.

(circumferential) elements. These are shown in figure 2. In the spanwise direction (fig. 2(a)) the first grid line describes the hub contour and the last is at the hypothetical outer casing. The first 20 grids in the spanwise direction are evenly spaced, with the 20th representing the blade tip. The remaining spanwise grids are spread somewhat. The streamline at the blade tip does not represent the true geometry of the tip. In the streamwise direction the blade leading and trailing edges are represented by the 10th and 30th grid lines, respectively. The distribution of the mesh in the pitchwise direction is shown at both the hub and blade tip (fig. 2(b)). The first pitchwise grid includes the suction side of the blade and the last includes the pressure side. The blade is so thin at the tip that it is unresolved in the figure.

The input options to the code were set for no swirl and no radial acceleration at the first upstream station. At the last downstream station the static pressure at the hub was set to 23 841.8 N/m^2, which is the static pressure at altitude. Several input options affect the convergence rate and stability of the solution. A variable time-step with a time-step multiplying factor of 0.35 was used. For stability a linear smoothing in the pitchwise and spanwise directions was used with a smoothing factor of 0.07. The relaxation factor on pressure corrections was 0.05, and the damping factor controlling the amount of negative feedback per iteration was set at 50. This particular combination of parameters was close to optimal and gave convergence on the Cray 1-S in about 800 sec of central processor time.

Of the many options for output from these calculations, results are shown for the relative Mach numbers, static pressures, and radial velocity components for both surfaces of the blade. Color contours for each variable are shown. The color bar indicates the linear relationship between the color shade and the intensity of each parameter within the extremes noted. Streamwise surveys are also shown for each variable at the hub, 88-percent span, and blade tip positions.

Relative Mach numbers on the suction and pressure sides of the SR-3 blade are shown in figure 3. Superimposed contour lines are shown at Mach numbers of 0.8, 1.0, and 1.2 on the suction side, and at 0.69 and 1.0 on the pressure side. The highest Mach number is slightly over 1.3 and occurs near the tip of the blade on the suction side. Both the pressure and suction sides show regions of high Mach number with the possibility of shocks near the hub, indicating that a design refinement would be beneficial. On the suction side, a rapid deceleration occurs near the trailing edge of the blade. This corresponds to a trailing-edge shock, although the velocity gradient is smeared out in this kind of calculation. The low-velocity zone near the leading edge in the region of the hub on the pressure side of the blade is a stagnation point, indicating that the blade is operating at an appreciable angle of attack.

Static pressure profiles (fig. 4) show low-pressure zones corresponding to the high-velocity zones. The trailing-edge shock is indicated again by the high positive pressure gradient near the suction-side trailing edge. The maximum pressure occurs in the stagnation region near the leading edge on the pressure side. The appropriate components of these pressures on both sides of the blade sum up the torque and thrust of the blade and determine the source strengths in the loading noise component of the acoustic field.

ORIGINAL PAGE
COLOR PHOTOGRAPH

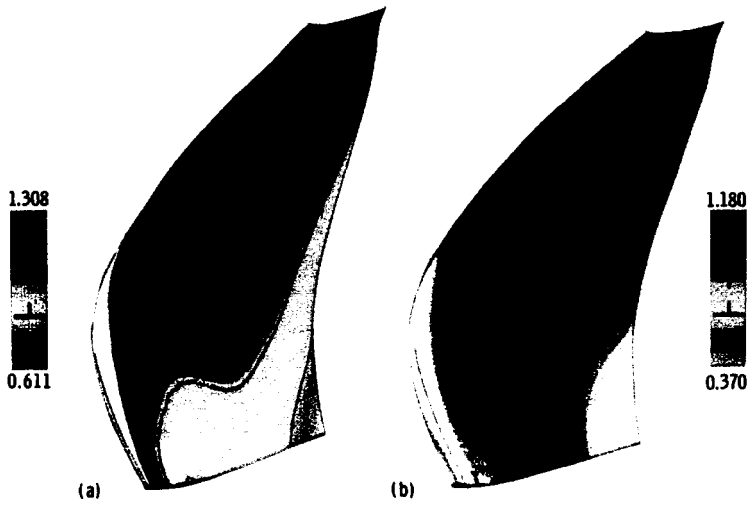

(a) Suction side.
(b) Pressure side.

Figure 3.—Relative Mach number contours for SR-3 blade.

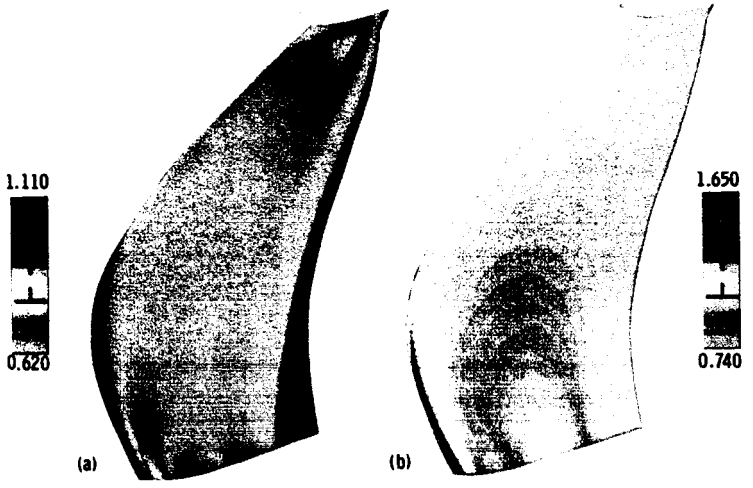

(a) Suction side.
(b) Pressure side.

Figure 4.—Static pressure contours for SR-3 blade.

Contours of the radial component of the velocity are shown in figure 5. The contour lines correspond to VR = 0 and 57 m/sec. Near the hub the flow is forced to spread radially outward on both sides of the blade by the hub shape. Near the end of the blade a tip vortex is indicated by the flow outward on the pressure side and flow toward the hub (negative radial velocity) on the suction side of the blade. The maximum radial velocity component is 87 m/sec, which is not large compared to the typical axial component of 250 m/sec. Hence, although these radial flows are important, the primary factor determining the pressures on the blade surfaces is the axial flow.

Surveys of the calculated relative Mach number and pressure on the surfaces of the blade are shown in figures 6 and 7. The surveys are in the streamwise direction at radial positions representing the hub (K = 1), 88-percent span (K = 17), and the blade tip (K = 20). These figures are a quantitative graphical representation of the same data as in figures 3 and 4. To give a better view of how the flow changes around the leading and trailing edges, two added points upstream of the

ORIGINAL PAGE
COLOR PHOTOGRAPH

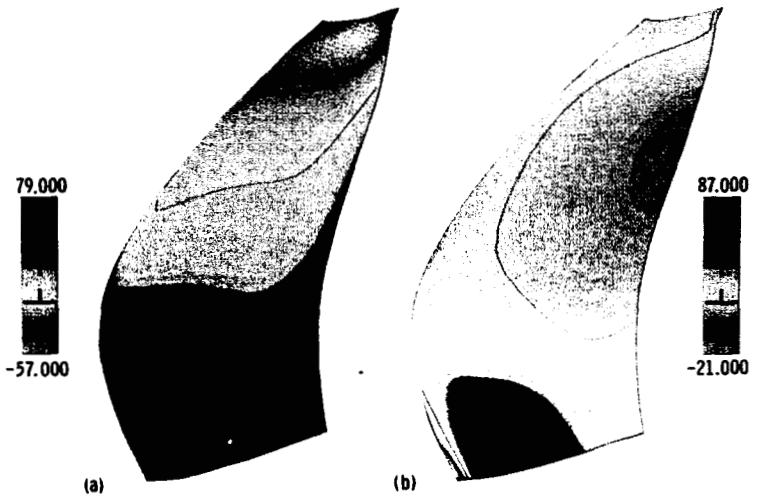

(a) Suction side.
(b) Pressure side.

Figure 5.—Radial velocity components for SR-3 blade.

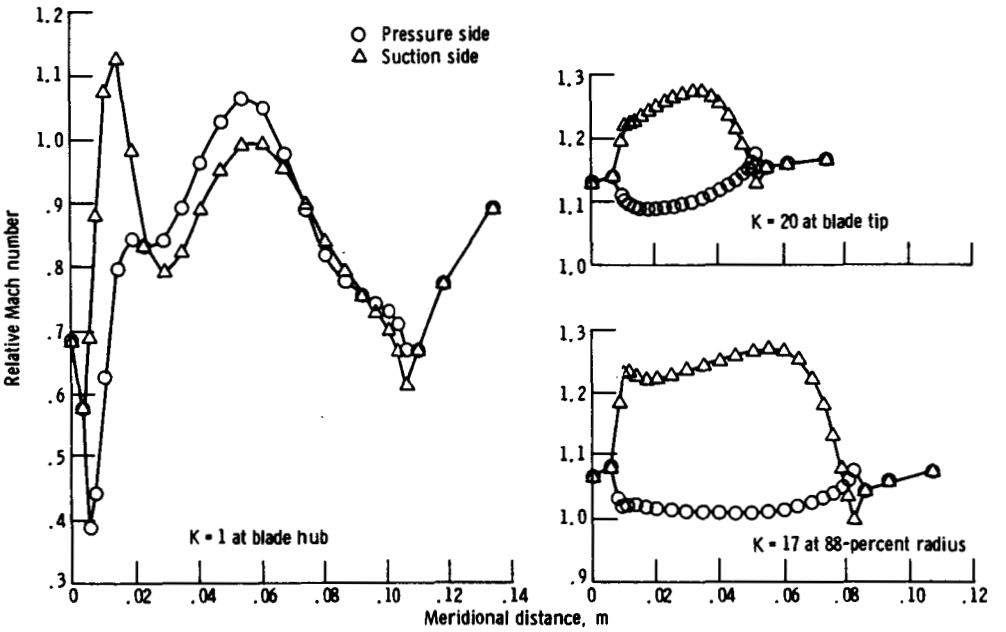

Figure 6.—Relative Mach number distribution for SR-3 blade surface.

blade and three downstream of the blade are shown. The same characteristics of the flow field can be seen as were noted before, i.e., the irregular flow near the hub, the trailing-edge shock, and a stagnation point on the pressure side near the leading edge. Again it should be noted that this finite-difference technique is unable to resolve the pressure and velocity discontinuities at a shock. The solution produces some "overshoot" in some cases, such as the first few grid points after the leading edge at 88-percent span, which may not represent true flow behavior.

Along with the aerodynamic solution results as exemplified by the previous discussion, the static pressures at each mesh point on the blade surfaces are normalized and saved in a separate file on the Cray 1-S for reading into the Farassat acoustic prediction program.

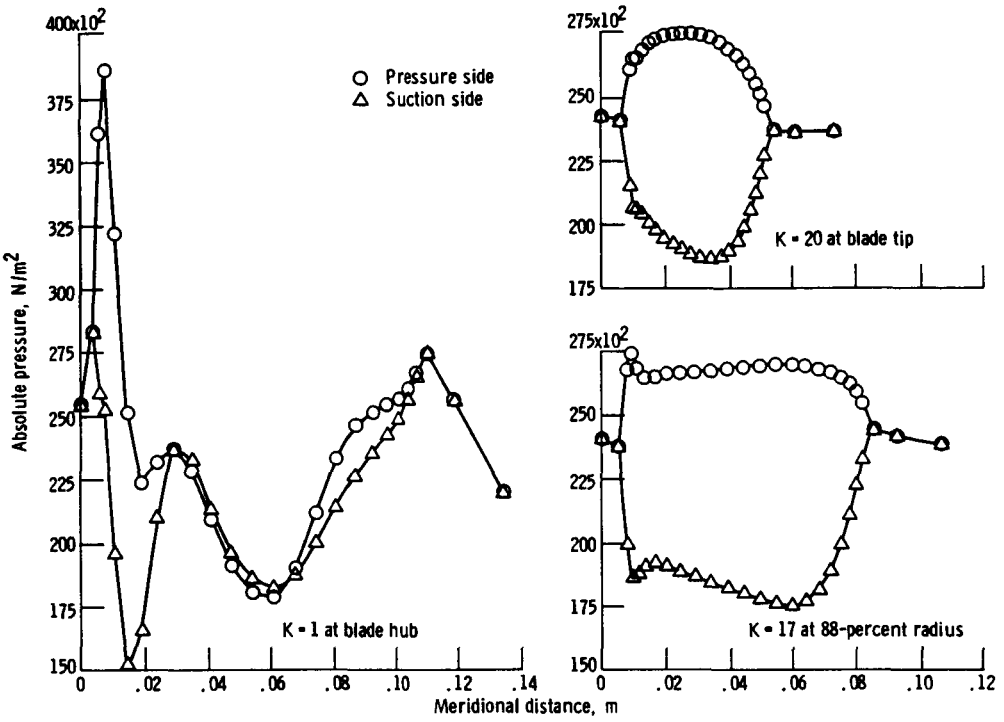

Figure 7.—Pressure distribution on the SR-3 blade surface.

Acoustic Calculations

The files of mesh coordinates and corresponding surface pressures from the Denton output are read as input to subroutine FUNPRES of the Farassat code. In addition, a separate file of blade coordinates is read in to describe the SR-3 blade shape in manufacturing coordinates; this file is read in subroutine FUNE2 for use there and by FUNE2Q. Other namelist-type inputs are used for the operating parameters and calculation options listed in table II.

The first page of output from the Farassat code is shown in table IV. It includes the value of the operating parameters and calculation options appropriate to the SR-3 design conditions. This output represents the acoustic calculations for a single observer station in the plane of the propeller, 0.81 m from the propeller axis (X0=0.81, 0.0, -0.01). Added calculations are required for other observer locations.

The input blade geometry assumes a blade setting angle of 60° at the 3/4 radius point (BETA34). The added input of OFFSET of -1.3° modifies this to the desired angle of 58.7°. For a flight speed of 237.3 m/sec and a propeller speed of 7348.5 rpm the resulting helical tip Mach number is 1.147, and for an 8-bladed propeller the blade passage frequency is 979.8 Hz. A total of 150 time points will be calculated within the period between blade passages of 0.0010206 sec. The indicator INDEXSL and other indicators at the bottom show how many times certain parts of some of the subroutines are called for the supersonic case. For reference purposes a line has been added at the bottom to show the parameters used in the Denton code when the pressure files were created.

Overall results are included in table IV. These include the calculated torque, thrust, and power input per blade. The power level of 14.58 kW/blade results from applying a correction factor (PFACTOR) of 0.910 to the pressures supplied by the Denton code. This factor is found by trial, and it is used to make the calculated power level match the design value. Subsequent acoustic calculations are based on these corrected pressures.

At this particular observer station the total noise of 141.72 dB is predominantly due to thickness noise rather than loading noise and hence will be somewhat insensitive to the pressure inputs. In most directions the loading noise is higher than the thickness noise: hence, the levels will be strongly dependent on the pressure distributions. For these calculations, no values were supplied for the surface friction on the blade so there is no calculated contribution by drag noise.

The results of calculating the predicted noise at several observer positions corresponding to microphone positions in the JetStar tests are shown in figure 8. In the tests eight microphones were placed on the fuselage 0.81 m below the propeller centerline. In addition, four microphones were located on an acoustic boom 0.81 m above the propeller centerline. All the microphone locations are given in table V. Measured data from these microphones were corrected to free-field conditions, based on reference 8; these corrections are also listed in table V. The corrections include the effects of

TABLE IV.—FARASSAT PROGRAM OUTPUT[a]

DATA SHEET SR3G.V1

OBSERVER IS IN MOTION.

C = 296.6 M/SEC
RHO = 0.3798 KG/M**3

XO = (0.81, 0.00, -0.01) M

V3 = 237.3 M/SEC
= 530.9 MPH

R = 0.317 M
RINNER = 0.093 M HELICAL M-TIP = 1.147

REV = 7348.5 RPM PER = 1.0206E-03 SEC
NBLADES= 8 BPF = 979.8 HZ

NPCA = 20 NPCAF = 3
NLE = 5 NCHF = 2
NTE = 10

OFFSET = -1.30 DEG. NTAU = 10
PFACTOR= 0.910
THKMXL = 0.05 DT = 6.8041E-06 SEC
FRACDT = 2.000
NPTS = 150 MTRANS = 0.950
NSPEC = 30 TRANS = 0.980
INDEXSL = 59991

EPSILON = 0.50 %

TORQUE = 18.95 N-M/BLADE
THRUST = 47.92 N/BLADE
POWER = 14.58 KW/BLADE

OASPL = 141.72 DB RE 20.E-6 PA
= 137.25 DB RE 20.E-6 PA (THICKNESS)
= 134.92 DB RE 20.E-6 PA (LOADING)
= -156.07 DB RE 20.E-6 PA (DRAG)

INDICATORS, NRTARD, NEEDTO = 397552 1234520 2102833 2102833
4880738 3348316 2921806 1 F

DENTON CALC. FOR 8 BLADES, RPM = -7348.5, INLET TOTAL
PRESS. = 36344.200 N/M**2, INLET VELOC. = 237.05 M/S,
DENSITY = 0.3796 KG/M

F. FARASSAT-P. NYSTROM
JIAFS-NASA/LARC-GWU

[a]First page only.

refraction in the boundary layer on the fuselage and of scattering at the surface of either the boom or fuselage. The flight conditions during the measurements were not precisely at design conditions, but the differences should have a small acoustic effect.

In the forward directions and at the maximum the corrected data from the fuselage microphones are in good agreement with the free-field predictions. The boom microphone data are somewhat higher. In the direction aft of the maximum, the theory predicts several decibels too high. The discrepancy is larger than the free-field corrections. The estimated correction for the 0.47 microphone location on the fuselage may be excessive.

In figure 9 the predicted relative contribution of loading noise and thickness noise are shown along with the predicted total. There is some inaccuracy between the sum of the two components and the total, which is due to the fact that time histories are generated for each component separately and for the total, and then the levels are found by a Fourier analysis of each. The thickness noise maximizes in the plane of the propeller, and the loading noise maximizes further downstream. At most angles the loading noise dominates.

Predicted and measured spectra in the plane of the propeller are shown in figure 10. As before, the predicted level of the first harmonic is somewhat lower than the measured value on the JetStar fuselage. The reference 8 corrections for boundary-

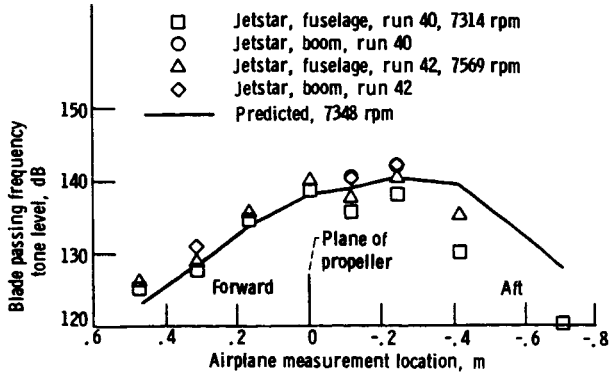

Figure 8.—Measured and predicted directionality of SR-3 blade passing tone for approximate cruise conditions. Measured flight data corrected to free-field by method of reference 8.

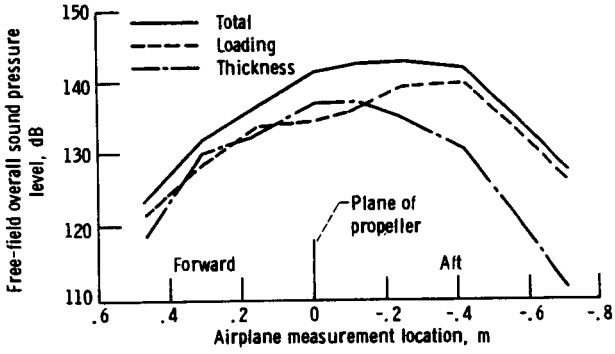

Figure 9.—Directivity of predicted loading and thickness noise for SR-3 propeller at design conditions.

layer refraction and reflections from the fuselage are small at this angle and have been neglected. At all harmonics the predicted thickness noise is higher than the loading noise by at least a decibel. It is also noteworthy that the measured

TABLE V.—BOOM AND FUSELAGE MICROPHONES FREE-FIELD CORRECTIONS[a]

Microphone	Axial position, m	Correction to free-field, dB
Fuselage 2	0.47	+20
3	.31	1.7
4	.16	-.5
5	-.01	-.8
7	-.25	-1.3
8	-.42	-3
9	-.71	-4.1
Boom 1	0.31	-2.3
[b]2	.16	-2.8
3	-.01	-3.2
4	-.25	-3.2

[a]From reference 8.
[b]Not functioning for these tests.

harmonics fall off at a higher rate than the predicted ones. This is at least in part due to the method of solution in the present form of the Farassat code. Revisions to the prediction code now in progress by Farassat (ref. 9) remove much of the high frequency "jitter" in the time history which shows itself in the higher harmonics.

The predicted spectrum at the position of the maximum loading noise is shown in figure 11. The thickness noise contributes little to the first two harmonic levels in this location. For the third and higher harmonics, the thickness noise is higher than the loading noise. The measured data at this angle include more high-frequency energy than do the data in the plane of the propeller. However, the predictions for this

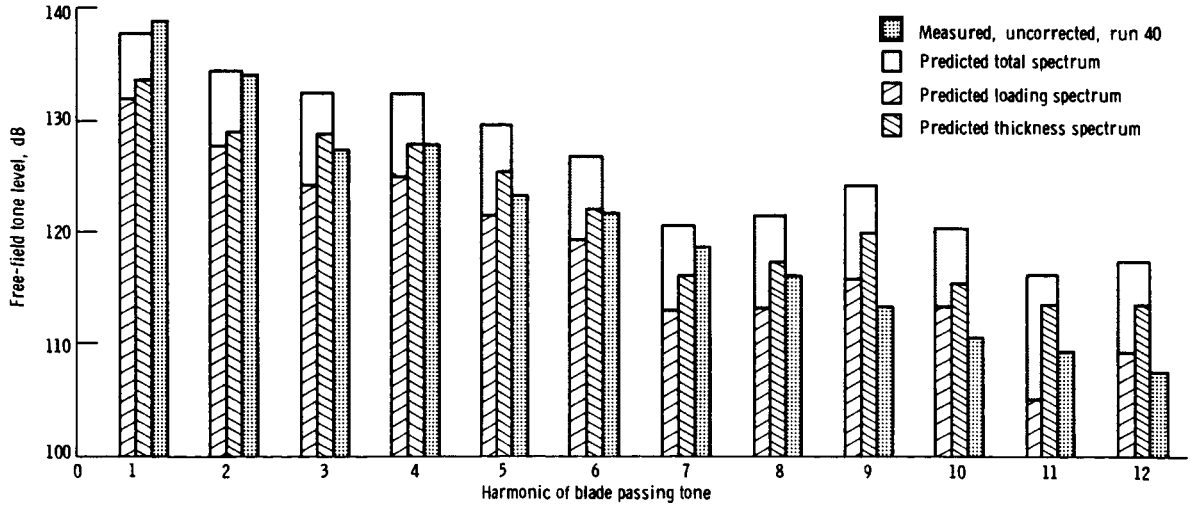

Figure 10.—Measured and predicted spectra at 0.81-m sideline in propeller plane.

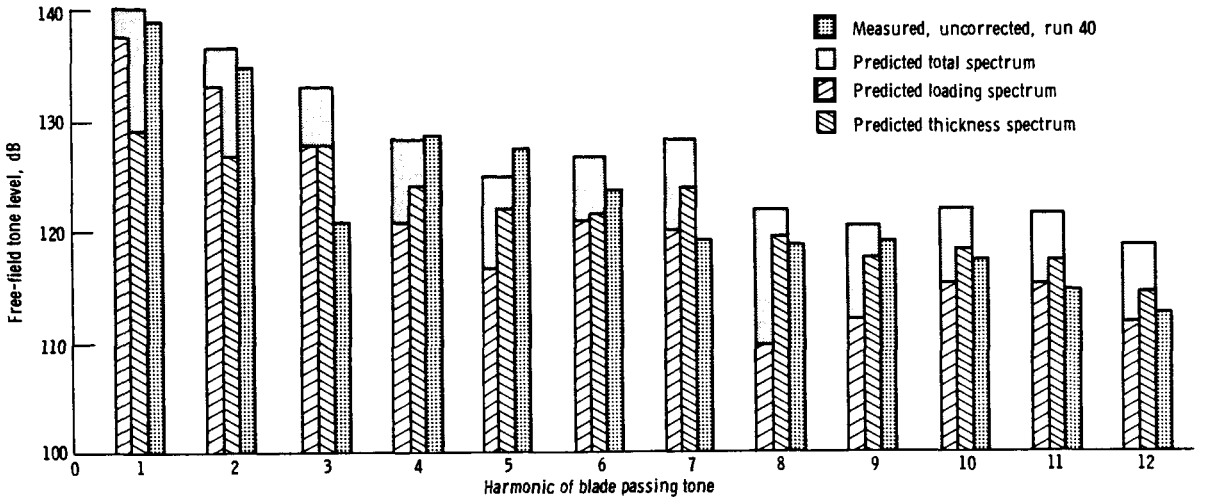

Figure 11.—Measured and predicted spectra at maximum loading noise location on 0.81-m sideline.

location still show more high-frequency content than the measured data.

Concluding Remarks

A procedure has been developed that is able to make both aerodynamic and acoustic predictions for a variety of turboprop blades, including the geometric complications of sources distributed over wide chords and highly swept tips. The inviscid aerodynamic code by Denton predicts the general features of the flow, including shocks and tip vortices, for a typical modern turboprop blade. The availability of color plotting routines is helpful in the assessment of the characteristics of the Denton code predictions and for observing particular features of the flow such as the shock locations and tip vortices.

In general, with aerodynamic predictions for the flow around the blades as input, the Farassat code gives a good prediction of the noise from a propeller at supersonic helical tip Mach numbers. However, some discrepancies between experimental measurements and predictions still remain. Efforts continue to evaluate the data from wind tunnels and JetStar flight tests, especially in correcting for the effects of the boundary layer.

Although the Denton code version with boundary-layer simulation is being incorporated in these predictions, preliminary evaluations indicate that there will be no great change in the general character of the flow. The effects reflect more than merely reducing the flow area near the trailing edge of the blade. The addition of mass at the blade surfaces to simulate the boundary layers affects the pumping effectiveness of the blade and therefore the velocities and pressures throughout the flow field.

No drag noise contribution was included in these Farassat noise calculations. It is possible that inclusion of a drag noise contribution could improve the match between the predictions and experimental data. It may also be that with shocks present the quadrupole terms should be added to the Farassat calculation of source strengths.

Lewis Research Center
National Aeronautics and Space Administration
Cleveland, Ohio, August 1985

References

1. Martin, R.M.; and Farassat, F.: User's Manual for a Computer Program to Calculate Discrete Frequency Noise of Conventional and Advanced Propellers. NASA TM-83135, 1981.
2. Denton, J.D., and Singh, U.K.: Time Marching Methods for Turbomachinery Flow Calculation. Application of Numerical Methods to Flow Calculations in Turbomachines, VKI-LEC-SER-1979-7, von Karman Institute for Fluid Dynamics, 1979.
3. Anderson, B.H.; Putt, C.W.; and Giamati, C.C.: Application of Computer Generated Color Graphic Techniques to the Processing and Display of Three-Dimensional Fluid Dynamic Data. Computers in Flow Predictions and Fluid Dynamics Experiments, K.N. Ghia, T.J. Mueller, and B.R. Patel, eds., ASME, 1981, pp. 65–72.
4. Dittmar, James D.: A Comparison Between an Existing Propeller Noise Theory and Wind Tunnel Data. NASA TM-81519, 1980.
5. Dittmar, James H.; and Lasagna, Paul L.: A Preliminary Comparison Between the SR-3 Propeller Noise in Flight and in a Wind Tunnel. NASA TM-82805, 1982.
6. Brooks, B.M.; and Mackall, K.G.: Measurement and Analysis of Acoustic Flight Test Data for Two Advanced Design High Speed Propeller Models. AIAA Paper 84-0250, Jan. 1984.
7. Neumann, H.E., et al: An Analytical and Experimental Comparison of the Flow Field of an Advanced Swept Turboprop. AIAA Paper 83-0189, Jan. 1983.
8. Hanson, D.B.; and Magliozzi, B.: Propagation of Propeller Tone Noise Through a Fuselage Boundary Layer. J. Aircr., vol. 22, no. 1, Jan. 1985, pp. 63-70.
9. Farassat, F.: A New Aerodynamic Integral Equation Based on an Acoustic Formula in the Time Domain. AIAA J., vol. 22, no. 9, Sept. 1984, pp. 1337-1340.

1. Report No.	2. Government Accession No.	3. Recipient's Catalog No.
NASA TM-87094		

4. Title and Subtitle	5. Report Date
Coupled Aerodynamic and Acoustical Predictions for Turboprops	March 1986
	6. Performing Organization Code: 505-45-58
7. Author(s): Bruce J. Clark and James R. Scott	8. Performing Organization Report No.: E-2688
	10. Work Unit No.
9. Performing Organization Name and Address: National Aeronautics and Space Administration, Lewis Research Center, Cleveland, Ohio 44135	11. Contract or Grant No.
	13. Type of Report and Period Covered: Technical Memorandum
12. Sponsoring Agency Name and Address: National Aeronautics and Space Administration, Washington, D.C. 20546	14. Sponsoring Agency Code

15. Supplementary Notes

Prepared for the One hundred and seventh Meeting of the American Acoustical Society, Norfolk, Virginia, May 7-10, 1984.

16. Abstract

To predict the noise fields for proposed turboprop airplanes, an existing turboprop noise code by Farassat has been modified to accept blade pressure inputs from a three-dimensional aerodynamic code. An Euler-type code written by Denton can handle the nonlinear transonic flow of these high-speed, highly swept blades. This turbofan code of Denton was modified to allow the calculation mesh to extend to about twice the blade radius and to apply circumferential periodicity rather than solid-wall boundary conditions on the blade in the region between the blade tip and the outer shroud. Outputs were added for input to the noise prediction program and for color contour plots of various flow variables. The Farassat input subroutines were modified to read files of blade coordinates and predicted surface pressures. Aerodynamic and acoustic results are shown for the SR-3 model blade. Comparison of the acoustic predicted results with measured data show good agreement.

17. Key Words (Suggested by Author(s))	18. Distribution Statement
Propeller aerodynamics Acoustics Computational fluid dynamics	Unclassified - unlimited STAR Category 02

19. Security Classif. (of this report)	20. Security Classif. (of this page)	21. No. of pages	22. Price*
Unclassified	Unclassified	11	A02

*For sale by the National Technical Information Service, Springfield, Virginia 22161